RESEARCH PAPER

Study on precise weld diameter validations by comparing destructive testing methods in resistance spot welding

Christian Mathiszik[1] · Johannes Koal[1] · Jörg Zschetzsche[1] · Uwe Füssel[1] · Hans Christian Schmale[1]

Abstract

The torsion test is rarely used for resistance spot-welded joints since they are not subjected to torsion in applications. Normal, shear, and/or peel loads are usually the main stresses. Extensive scientific investigations in the context of Kunsmann's dissertation date back more than 50 years. These investigations are still the basis of ISO 17653 and the German guideline DVS 2916-1. Recent scientific investigations only use torsion tests, but do not describe the reason for its use. A decisive advantage of the torsion test over the other standardized destructive testing methods lies in the types of fracture modes that occur and the properties of the fracture surfaces. Torsional loading results in either interfacial or button-pulled fracture modes. No material residues occur on the fracture surfaces for ductile and advanced high-strength steels. Hence, the measurement of weld diameter is achievable with minimal constraints, resulting in reduced variability and facilitating objective assessments of spot welds. This article delineates these attributes through a comparative analysis of various destructive testing methods employing statistical approaches. Additionally, the article expounds on the design concept of the developed rig for conducting torsion tests on spot welds.

Keywords Resistance spot welding · RSW · Torsion test · Chisel test · Shear tensile test · Cross tensile test · Destructive testing · Automated testing · Spot welds · NDT · FEM · DVS 2916 · ISO 10447 · ISO 14273 · ISO 14372 · ISO 17653

1 Introduction

Resistance spot-welded joints are widely used in the sheet metal processing industry. Applications can be found wherever sheets with thicknesses of up to approx. 3.0 mm are

---

Recommended for publication by Commission III - Resistance Welding, Solid State Welding, and Allied Joining Process.

✉ Christian Mathiszik
christian.mathiszik@tu-dresden.de

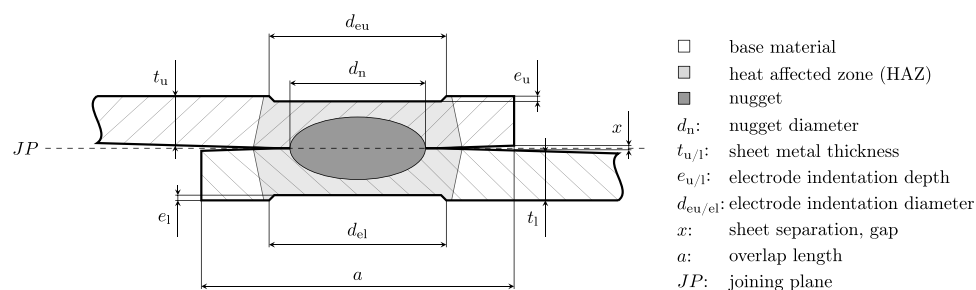Johannes Koal
johannes.koal@tu-dresden.de

Jörg Zschetzsche
joerg.zschetzsche@tu-dresden.de

Uwe Füssel
uwe.fuessel@tu-dresden.de

Hans Christian Schmale
hans_christian.schmale@tu-dresden.de

[1]   Chair of Joining Technology and Assembly, Technische Universität Dresden, Helmholtzstr. 5, Dresden 01069, Germany

elementally welded together. These include vehicle and metal constructions, the furniture industry, and applications in electrical engineering. Resistance spot welding RSW already achieves high reliability when joining conventional steels, such as mild steels. In the automotive industry, the trend towards high-strength and ultra-high-strength steels in the body-in-white production for safety-relevant structures continues unabated. In addition, lightweight construction is striving to reduce CO_2 emissions and material input. These factors lead to smaller process windows and higher challenges in terms of process control, process reliability, and quality assurance in RSW. The most important parameters for quality assurance are the nugget diameter d_n and the weld diameter d_w. Both describe the geometric expansion of the welded joint. The difference between both lies in the method of determination. The nugget diameter d_n can only be measured on metallographic cross-sectional specimens. The weld diameter d_w is measured by all other methods of DT. A ratio of $d_w = 1.15 d_n$ can be assumed for ductile materials [1]. Due to the process characteristics and as illustrated in Fig. 1, the welded joint is not visible from the outside and cannot be assessed by visual, magnetic particle, or dye pen-

Fig. 1 Schematic illustration of a spot-welded joint of two sheets and the main geometrical parameters

□ base material
□ heat affected zone (HAZ)
▣ nugget
d_{n}:   nugget diameter
$t_{\mathrm{u/l}}$:   sheet metal thickness
$e_{\mathrm{u/l}}$:   electrode indentation depth
$d_{\mathrm{eu/el}}$: electrode indentation diameter
x: sheet separation, gap
a: overlap length
JP: joining plane

etrant inspection. Thus, neither d_{n} nor d_{w} can be measured directly. This causes serious challenges for non-destructive testing (NDT) regarding accuracy and the resulting confidence of the NDT systems.

2 Spot weld validation methodologies

According to guideline DVS 2916-5 [2], which reflects the current state of the art in NDT of RSW, three methods are available for quality assurance:

1. Process monitoring during the welding process
2. Process control during the process
3. Quality inspection after the process

Process parameters are recorded and analyzed at the first two methods. They provide indications of process variations and/or intervene directly into the process. Neither of these methods can be regarded as NDT methods since they do not permit direct evaluation of the welded joint. For this reason, additional random DT and/or NDT of the welded joints are carried out. Possible NDT methods are described in detail in guideline DVS 2916-5 [2]. Manual ultrasonic testing is the most widely used testing method among the methods discussed in this guideline. In principle, thermography, active or passive, and pMFT [3–6] are also suitable, but their implementation into industrial series applications is not given yet. All these NDT methods are indirect ones, requiring a reference or comparable parameter for the evaluation, validation, and calibration. In general, the reference parameter, e.g., the spot weld diameter d_{w}, is determined experimentally. For this purpose, a series of spot welds with the aim of increasing nugget size is produced. The welds are tested non-destructively and destructively. The results are compared to each other. Commonly chisel tests are chosen for this procedure. It is well known that chisel tests require a high level of force, which carries a significant risk of injury. It is also labor- and time-intensive and does not allow data acquisition during the test. Further and often used possible DT methods are analyses on metallographic cross-sections, tensile-shear, cross-tension, and peel tests. Based on numerous publications, it can be stated that usually the current available or easy

applicable DT methods are used without further questioning of their suitability for the validation of the NDT results. This is evident across all NDT methods, where the most frequently studied methods are thermography [7–10], ultrasonic testing [11–31] and parameter monitoring/analysis, data mining, and methods of artificial intelligence [12, 18, 32–38]. In none of these publications, the choice of the DT method is justified, or a statistical evaluation of the DT results is provided. The results are evaluated and accepted uncritically as correct. However, it is well known that the measurement procedure of the spot weld diameter d_{w} depends on the personnel experience, the measuring equipment, the ambient light conditions, and the fracture characteristics. The latter are mainly determined by the deformation that occurs and by potential remaining material around the weld diameter d_{w}. Thus, considerable uncertainties must be expected. For these reasons, NDT results often correlate only roughly with the DT results. This becomes evident in [39], which states that the results of shear-tensile tests correlate only slightly, those of peel tests barely, and those of chisel tests not at all with the results of manual post-process ultrasonic testing. Results of the individual DT methods correlate only slightly among each other [39]. These poor correlations reduce confidence in current and new NDT systems, leading to significant uncertainty and resulting in an increased effort of DT [40]. This low confidence is highlighted in a recent survey by Deutsche Gesellschaft für Zerstörungsfreie Prüfung DGZfP. The authors state that the confidence in these systems is currently not very high due to the lack of standards and methods to determine the reliability of the newly developed NDT methods [41].

For these reasons, the alternative of torsion testing was considered at the Technische Universität Dresden. However, the torsion test is rarely used for spot welds. This is primarily attributed to the nature of stress encountered by spot welds in practical applications, where they are typically exposed to normal, shear, peel, or a combination of these loads, rather than torsional stress due to the specific joining geometry. Guideline DVS 2902-3 [1] explicitly states that spot welds should not be subjected to torsional stress, as only small loads can be transmitted. Extensive scientific investigations of torsion testing in the context of Kunsmann's dissertation date back more than 50 years. These investigations are still the basis of ISO 17653 [42] and the German guideline DVS 2916-

Table 1 Destructive testing methods with associated standards and selected specimen geometries for the investigations

DT-ID	DT method	Standard	Geometry (width × length)	Overlapping area
CT	Chisel test	ISO 10447	50 mm × 50 mm [1]	40 mm × 50 mm[1]
TST16			50 mm × 170 mm	16 mm × 50 mm[2]
TST35	Tensile-shear test	ISO 14273	50 mm × 170 mm	35 mm × 50 mm
CTT	Cross-tension test	ISO 14272	60 mm × 140 mm	60 mm × 60 mm
TT (60×40)	Torsion test	ISO 17653	60 mm × 40 mm	60 mm × 40 mm
TT (50×50)			50 mm × 50 mm [3]	50 mm × 50 mm [3]

[1]In accordance to SEP 1220-2 [46]

[2]Common flange widths in automotive engineering [45]

[3]Geometry for investigations of the effect of sample geometry at torsion test

1 [43]. Both standards distinguish between non-instrumented (workshop test) and instrumented torsion tests. This paper focuses on the instrumented torsion test, where the torque is continuously recorded over the torsion angle during the test sequence. The angular velocity ω influences the test result [43] and is quantified with 90° over approximately 5 s in ISO 17653 [42]. The influence is not described in detail in either source. Recent scientific investigations in [44, 45] only use the torsion test, but do not describe the aim and reasons for its use.

In this article, the described inadequacies will be considered in more detail. Comparisons between the different DT methods in RSW are discussed, and the potential suitability of torsion testing with a specially developed test rig is presented in more detail. The specifications of the standards ISO 17653 [42] and DVS 2916-1 [43] concerning the angular velocity are addressed. Recommendations on setting parameters and possible specimen geometries for automated torsion testing are presented.

3 Materials and methods

3.1 Material combinations

The comparison of the different DT methods among each other is performed using tensile-shear, cross-tension, and torsion tests as instrumented and the chisel test as non-instrumented methods. Table 1 shows the test methods with

their corresponding internationally applicable standard and the specimen geometries used for the tests. For the tensile-shear tests (TST) and torsion tests (TT), alternative specimen geometries are used in addition to the standard specimens. For TST, the edge distance of the spot weld is 8 mm instead of 17.5 mm resulting in a smaller overlapping length of 16 mm instead of 35 mm. This considers the flange widths commonly used in the automotive industry [45]. The second specimen geometry for TT is intended to ensure that deviations in the specimen dimensions do not influence the test results. The reason for this is that the selected square specimen geometry is also suitable for chisel specimens according to SEP 1220-2 [46]. This enables a reduction in sample geometry diversity. Two MC are selected, representing ductile and brittle spot welds of steel. The ductile MC1 consists of two galvanized HX340LAD+Z100 sheets. The brittle MC2 is of two hot-stamped steel sheets of 22MnB5+AlSi with an aluminum-silicon coating. The selected sheet thicknesses t are 1.0 mm and 2.0 mm for both material combinations. Table 2 shows the selected MC in detail and the main welding parameters aiming a weld diameter $d_w = 5.0\sqrt{t}$, where t represents the sheet thickness of the thinner sheet of each MC. The squeeze and hold time are set to 400 ms. The welding parameters are determined previously by weldability lobes. The samples are welded with a C-type servo-electric welding gun with a stiffness $k = 2.345\ \mathrm{kN\,mm^{-1}}$. The welding current I_w is provided and controlled by a 1000 Hz medium-frequency-inverter using a constant current control. A detailed description of the welding test rig can be found

Table 2 Material combinations and welding parameters

MC	Material	Sheet thickness Upper t_u (anode)	Lower t_l (cathode)	Welding parameters Electrode force F_{el}	Weld time t_w	Weld current I_w
MC1	HX340LAD+Z100	1.0 mm	2.0 mm	2.7 kN	380 ms	8.0 kA
MC2	22MnB5+AlSi[1]	1.0 mm	2.0 mm	2.3 kN	700 ms[2]	6.4 kA[3]

[1]Hot-stamped condition

[2]Pre-pulse weld time $t_{w.pp} = 200$ ms

[3]Pre-pulse weld current $I_{w.pp} = 4.0$ kA

in [47]. The welding specimen production sequence is randomly designed within each MC to keep external influences, such as electrode wear or cooling water temperature fluctuations, to a minimum. Ten weld specimens are investigated for each MC and test parameter. After welding, all samples are destructively tested by the respective DT method and the fracture characteristics are evaluated. The comparison of the investigated DT methods is performed based on accessibility and the resulting measurability and measurement possibility of the weld diameter d_w. In most applications, a manual measurement is carried out using a caliper gauge according to ISO 10744 [48], as it is used for these investigations. Further, the results of the weld diameter d_w measurements are compared with the nugget diameters d_n determined on the metallographic cross-section (CS) of ten samples of each MC. A statistical non-parametric Mann–Whitney U test is used to identify the suitable DT methods that are applicable for validating NDT results. These should not show significant differences to the nugget diameters. The cross-section specimens are prepared according to DVS 2916-4 [49].

3.2 Test rigs for instrumented shear and head tensile tests and chisel tests

A Zwick Roell Z 030 testing device with a maximal tensile force of 30 kN is used for the instrumented tensile-shear and cross-tension tests. The manual chisel tests are performed using a recessed chisel according to ISO 10447 [48]. The specimens are clamped in a manual machine vice.

3.3 Developed test rig for instrumented torsion tests

The developed torsion test rig shown in Fig. 2 is characterized by a floating bearing on both sides of the specimens. This concept of bearing enables an automatic alignment of the clamped specimen around the axis of rotation of the spot weld. This ensures to be within the close tolerance of axis alignment of 0.5 mm according to ISO 17653 [42]. The floating bearing of the lower specimen holder is realized by a cross table. The upper specimen holder is connected to the drive shaft and consists of a double Cardan joint. This joint has a degree of freedom in a vertical direction (z) to compensate height changes due to lateral movements of the specimens while it aligns itself around its axis of rotation. The test rig enables the automated destruction of weld specimens with a constant and controlled angular velocity ω and continuous torque measurement M_T over the torsion angle φ. The constant angular velocity allows quasi-static torsion tests. The characteristics of the test rig are summarized in Table 3. During commissioning of the test rig, the angular velocity ω with 90° over approximately 5 s ($\omega = 3.0\,\mathrm{min}^{-1}$) as recom-
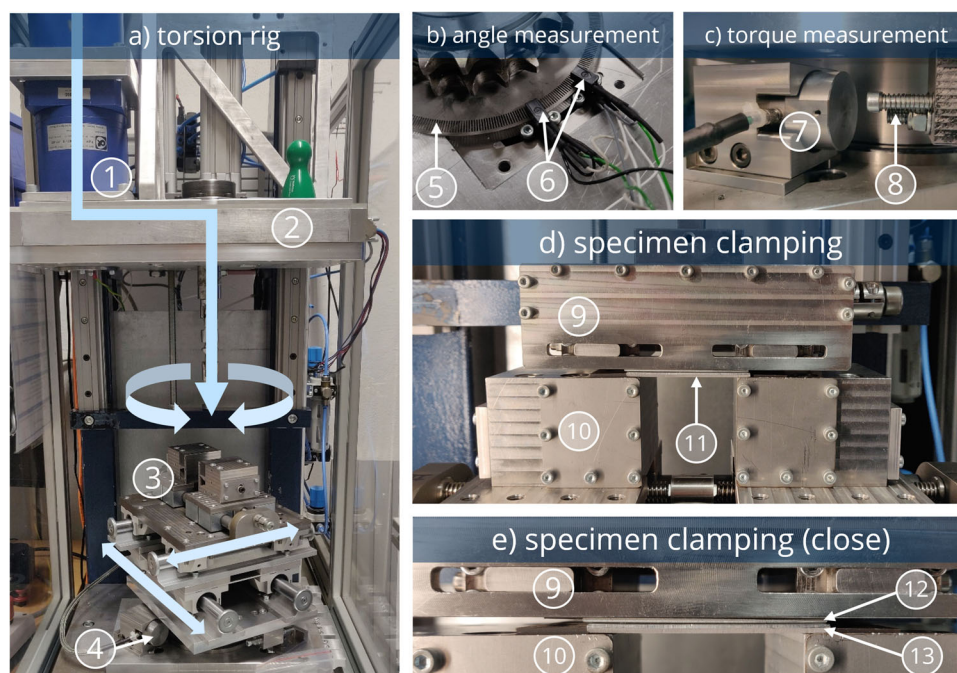
Fig. 2 Test rig for instrumented torsion testing at the Chair of Joining and Assembly Technology, Technische Universität Dresden, with a representation of the course of motion in **a** applying the torque on the specimens ((1) drive with two planetary gear units (ratio: 1:10, each); (2) housing for chain drive with angle measurement; (3) lower specimen clamping with floating bearing realized by a cross table; (4) torque mea-surement unit realized by a piezoelectric force sensor combined with the lever arm; **b** angle measurement with (5) incremental disc and (6) two photoelectric sensors; **c** torque measurement with (7) piezoelectric force sensor; (8) stop bolt; **d**, **e** specimen clamping with (9) upper sample holder (rotating); (10) lower sample holder (stationary); (11) specimen; (12) upper sheet; (13) lower sheet)

Table 3 Characteristics of the torsion test rig

Description	Key data
Max. torsional moment $M_{T.max}$	$250\,N\,m$
Angular velocity ω	$0–25\,min^{-1}$
Data acquisition	$M_{T.max}, \varphi$
Measurement frequency	$2000\,Hz$

mended in ISO 17653 [42] was considered too high, since the test procedure cannot be classified as quasi-static due to the high change in speed at the beginning of the test resulting in inconsistent strain rates. As a result, the angular velocity is set to $\omega = 0.3\,min^{-1}$ for these and further investigations. This provides comparable strain rates as tensile-shear or cross-tension tests.

4 Results

4.1 Comparison of DT methods

The instrumented DT methods provide different results for both MC. Figure 3 shows the maximum loads determined for the corresponding tests with F_{max} for the CTT, TST16, and TST35. The maximum measured torques M_{max} are shown for the TT-tests. Moderately different maximum forces are measured for MC1 depending on the test method. For MC2, a clear difference between the CTT and TST specimens can be observed, depending on the fracture characteristics due to the applied load of the respective test method. Very low scatter can be noted for both MC and TST16 and for MC1 and TST35. Larger scatter can be seen for the torsion specimens.

4.2 Characterization of fractures

The comparison of the DT methods indicates differences for both MC. All specimens fail by button-pulled fracture mode. All specimens of MC1 material remain on all fractures, except those of the torsion tests (see Table 4). Since the welds fail as brittle fractures due to lower material ductility at MC2, less material covers the weld diameter. The angular covering portion α_i of each sample is evaluated around the spot weld. The index i represents the number of the portion, if multiple separate material residues occur. Figure 4 shows representative examples of MC1, CTT, and TST35 as ductile fractures and an example of a brittle fracture of MC2, CTT, and sample 07. The evaluation of α_i is shown in Fig. 5 for each DT method for both MC. For MC1, the material residues cover almost half of the weld diameter of each sample except those of the torsion tests. For MC1, TST35 seven out of ten samples are covered completely. Material residues occur only at the tensile-shear tested samples at MC2.

4.3 Comparison of weld diameters

Figure 6 shows the measured weld diameters d_w for each DT method of MC1 and MC2. The weld diameters of MC1 differ strongly between the DT methods. The comparison with the mean value of the nugget diameters $d_{n.mean}$ emphasizes these differences. This particularly applies to the comparison of the tensile-shear tests with those of the torsion tests, as the mean values of the tensile-shear tests ($d_{w.mean}$ (SST35) $=$ 10.14 mm; $d_{w.mean}$ (SST16) $=$ 9.67 mm) are much larger than those of the torsion tests ($d_{w.mean}$ (TT (60 x 40)) $=$ 6.3 mm; $d_{w.mean}$ (TT (50x50)) $=$ 6.14 mm). These differences can be attributed to the resulting fracture modes of the specimens. MC2 shows a completely different behavior compared to MC1. The measured weld diameters d_w in Fig. 6 are much closer to each other and have lower variances.

In general, it can be stated that the portion of the material residues α_i affects the accuracy of the weld diameter measurement according to ISO 10447 [48]. The larger the portion α_i, the lower the accuracy of the measurement and the larger the differences to the respective nugget diameters, as the material residues impede the accessibility with the caliper measuring tips.

Fig. 3 Measured maximum loads F_{max} and M_{max} occurring during DT for MC1 (left) and MC2 (right)
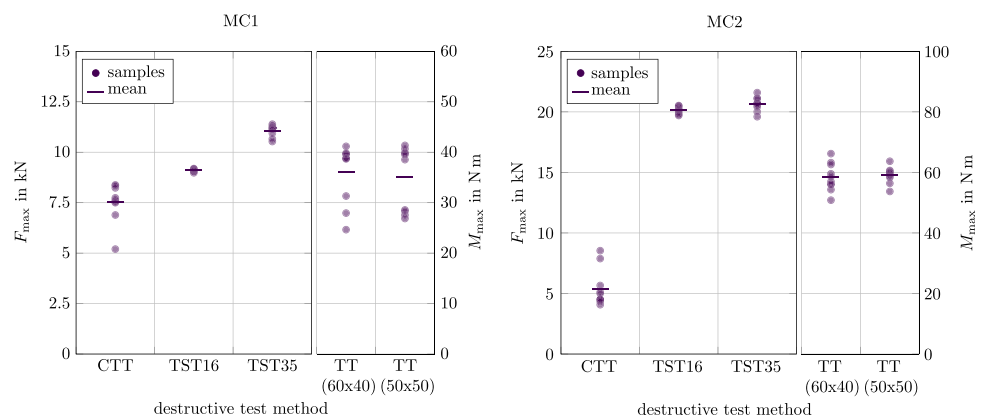
Table 4 Evaluation of the fracture surfaces of the individual DT methods with an indication of the fracture mode and the ratio of material residues on the fracture covering the weld diameter

MC	DT-ID	DT method	Fracture modes	Covering material residues
MC1	CT	Chisel test	100% button-pulled	10/10 samples
	TST16		100% button-pulled	10/10 samples
	TST35	Tensile-shear test	100% button-pulled	10/10 samples
	CTT	Cross-tension test	100% button-pulled	10/10 samples
	TT (60×40)	Torsion test	100% button-pulled	0/10 samples
	TT (50×50)		100% button-pulled	0/10 samples
MC2	CT	Chisel test	100% button-pulled	0/10 samples
	TST16		100% button-pulled	9/10 samples
	TST35	Tensile-shear test	100% button-pulled	7/10 samples
	CTT	Cross-tension test	100% button-pulled	0/10 samples
	TT (60×40)	Torsion test	100% button-pulled	0/10 samples
	TT (50×50)		100% button-pulled	0/10 samples

5 Discussion

The results of the DT method comparison show differences depending on the material used. The more ductile the material, the higher the risk of material remaining on the fracture surface of the specimen after DT. Hence, a comparison of the measured maximum forces F_{max} and torques M_{max} is not practical at this point, as all samples fractured in the sheet metal and not in the spot weld. Together with the measured weld diameters d_w, this results in incorrect and misleading strength considerations, especially at those samples with residual material at the fracture. The button-pulled fractures always result in material residues on the fractures for the DT methods CT, TST, and CTT and ductile materials. From the tensile strength testing point of view, these material residues are acceptable. In the case of a button-pulled fracture, it can be assumed that the spot weld has sufficient geometric dimension, as it is required. For brittle materials, this aspect cannot be stated so clearly, as the results show.

To determine significant differences of the DT methods, a statistical analysis is performed using the non-parametric Mann–Whitney U test, which refers to the nugget diameters d_n. The test is also used to compare the influence of the sample geometry between TT (60×40) and TT (50×50). This test method is used since a normal distribution of the samples cannot be assumed for all DT methods. The following hypotheses are defined:

H_0 There are *no* difference between the nugget diameter d_n and the weld diameter d_w of the respective DT method.
H_1 There are difference between the nugget diameter d_n and the weld diameter d_w of the respective DT method.

The data for group 1 are the ten ($n_1 = 10$) nugget diameters d_n and for the respective second groups the ten ($n_2 = 10$) weld diameter d_w of the respective DT method and MC. The data of both groups is classified into ranks. This results in the rank sums R_1 and R_2 for group 1 and group 2. The test statistic U_1 and U_2 is calculated by Eqs. 1 and 2. H_0 is rejected if $\min[U_1, U_2] \leq U$, where U is the critical value according to the Mann–Whitney U table. $U = 23$ with the chosen significance level $\alpha = 0.05$ and ($n_1 = n_2 = 10$).

$$U_1 = n_1 n_2 + \frac{n_1(n_1+1)}{2} - R_1 \tag{1}$$

$$U_2 = n_1 n_2 + \frac{n_2(n_2+1)}{2} - R_2 \tag{2}$$

The evaluation of the test can be seen in Table 5. The individual test results are in Tables 4 and 7. For MC1, statistically significant differences (H_0 rejected, H_1 accepted) can be
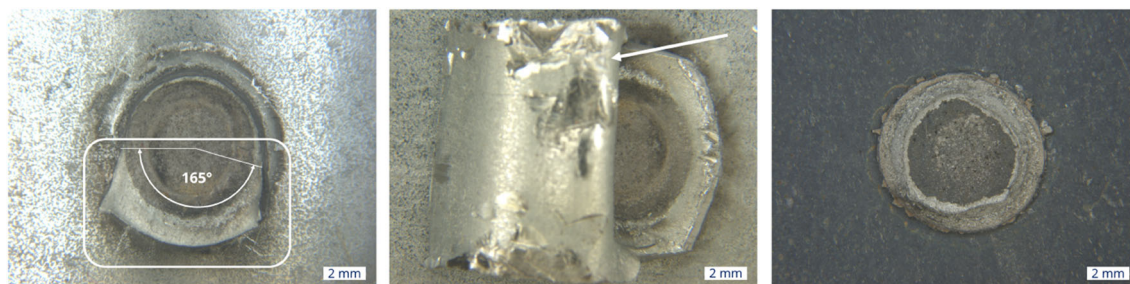
Fig. 4 Fracture images of destructive tested samples of MC1 (CTT, sample 07) (left) and MC1 (TST35, sample 07) (middle) with indications of the covering residual material portion α_i at the fractures and MC2 (CTT, sample 07) as an example of a sample without any covering residue material (right)

Fig. 5 Angular portion α_i of the covering material residues on the fractures of each sample and DT method for MC1 (left) and MC2 (right)


6 Conclusion
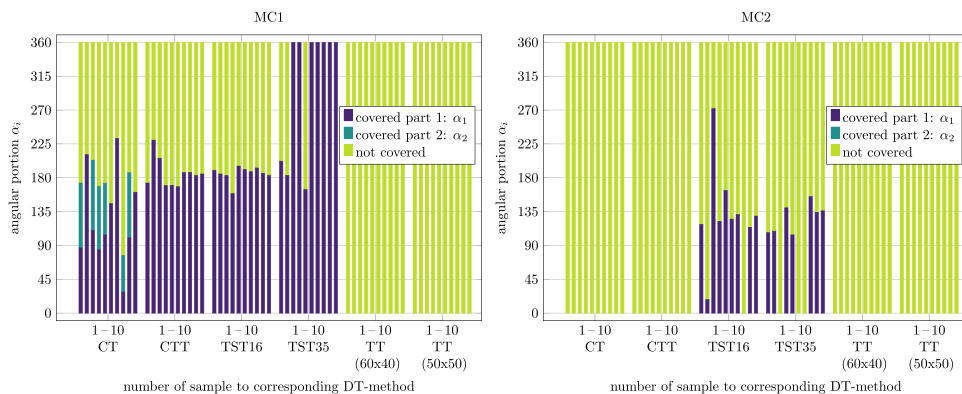
assumed for CT, CTT, TST16, and TST35. For MC2, this applies to CTT, TST16, and TST35. There are no statistically significant differences in the results of the diameter determination for TT, for MC2, and also for CT. H_0 is accepted. When applying the ratio of $d_\mathrm{w} = 1.15 d_\mathrm{n}$ according to [1] for CT of MC1, the differences are not significant and H_0 is accepted. This does not apply to the weld diameters of the other DT methods CTT, TST16, and TST35. The different geometric sample dimensions of the TT specimens also show no statistically significant differences. For all DT methods, where H_0 is rejected, material residues occurred on the fractures of these specimens. This material prevents precise measurements, especially for MC1 as a ductile material combination. This is also shown by the results of the weld diameter, which seem to be much larger, although the same welding parameters were used for all specimens within each MC. Thus, strongly deviating diameters were determined, which probably do not have much in common with the real weld diameter. When looking at the specimens after DT, all specimens show significant deformations, except for the TT specimens. Here, the sheets remain flat and do not show any changes in shape. This is another indication of the good suitability for validations of the weld diameter, since no energy goes into the specimen deformation—any deformation up to fracture takes place in the spot weld.

The literature research revealed one main problem: little or no attention is paid to whether the selected DT method is suitable for a good validation of the NDT results or the parameter analysis at all. The suitability of a DT method must be derived from the NDT results. For example, modern ultrasonic test systems for RSW provide the welded surface in the joint planes as a result. However, this surface can only correlate with the forces at fracture if the force is applied as normal force on the joint plane. In the case of a button-pulled fracture, no correlations can be derived. When comparing the fracture surfaces with the determined NDT areas, it is important to ensure that no material residues are present on the fractures for a precise measurement of the weld diameter or the weld area. These requirements are met by the torsion test, in which no material residues occur at the fractures in either ductile or brittle material. The specimens do not deform in the sheet metal plane and are therefore very well suited for further examinations such as microscope images, since no great demands are made on depth of focus. The sample preparation and test procedure is simpler compared to the other DT methods of this article. From the perspective of spot weld testing in the field of research and development and for the validation of weld tests and NDT systems as well as FEM

Fig. 6 Weld diameters d_w measured manually by caliper of the investigated DT methods for MC1 (left) and MC2 (right) in comparison with the nugget diameter d_n
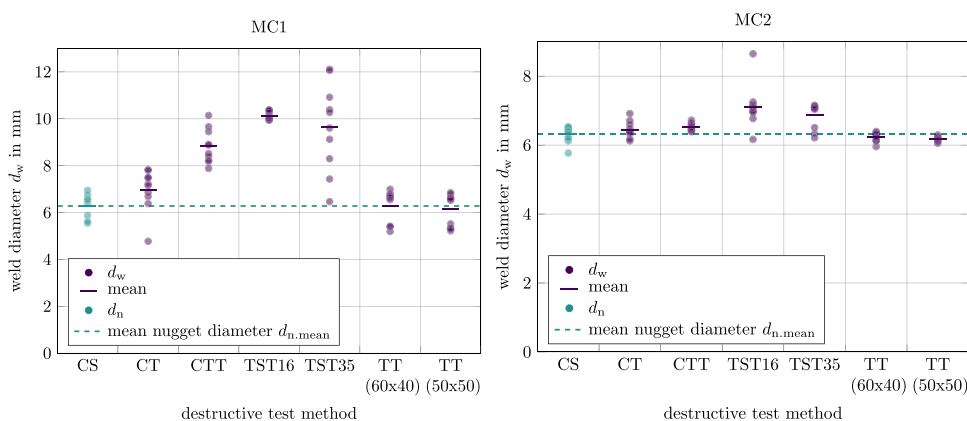
Table 5 Evaluation of the Mann–Whitney U test for MC1 and MC2 of the weld diameter d_w of the different DT methods in relation to the nugget diameter d_n (CS) and the comparison between the TT geometries

MC	DT-ID 1	DT-ID 2	R_1	R_2	U_1	U_2	Min(U_1, U_2)	H_0/H_1
MC1	CS	CT	138	72	17	83	17	H_1
MC1	CS	CT[1]	98	112	57	43	43	H_0
MC1	CS	CTT	155	55	0	100	0	H_1
MC1	CS	TST16	155	55	0	100	0	H_1
MC1	CS	TST35	151	59	4	96	4	H_1
MC1	CS	TT (60×40)	112	98	43	57	43	H_0
MC1	CS	TT (50×50)	103	107	52	48	48	H_0
MC1	TT (60×40)	TT (50×50)	93	117	62	38	38	H_0
MC2	CS	CT	115	95	40	60	40	H_0
MC2	CS	CTT	136	74	19	81	19	H_1
MC2	CS	TST16	147	63	8	92	8	H_1
MC2	CS	TST35	140	70	15	85	15	H_1
MC2	CS	TT (60×40)	87	123	68	32	32	H_0
MC2	CS	TT (50×50)	80	130	75	25	25	H_0
MC2	TT (60×40)	TT (50×50)	89	121	66	34	34	H_0

[1]With ratio of $d_w = 1.15 d_n$ according to [1]

models, there are several reasons for using torsion testing on spot-welded joints that can be summarized:

1. Torsion test requires small sample geometries compared to other instrumented DT methods for RSW like tensile-shear or cross-tension test.
2. Torsion-tested specimens show low deformations.
3. Fracture behavior and the advantages thereof.
4. No material residues around the fracture surface allowing precise measurements of the weld diameter
5. Defined stress due to torsion.

The authors of this article emphasize that the above-mentioned reasons using this DT method for spot welds should be considered more often in future investigations, especially when validating methods of non-destructive quality assurance or numerical models, e.g., by FEM.

Appendix: A Measured diameters and ranks for the Mann–Whitney *U* test

Table 6 Nugget diameters $d_{n.i}$ and weld diameters $d_{w.i}$ of each sample

MC	DT-ID	$d_{w.i}$, $d_{n.i}$ of samples in mm										d_{mean} in mm
		1	2	3	4	5	6	7	8	9	10	
MC1	CS	6.26	6.30	5.62	6.56	6.55	5.55	6.95	6.76	6.38	5.88	6.281
MC1	CT	6.38	7.83	7.15	6.69	7.81	7.22	4.78	7.50	6.87	7.48	6.969
MC1	CT[1]	5.55	6.80	6.22	5.81	6.79	6.28	4.15	6.52	5.97	6.50	6.060
MC1	CTT	7.88	8.22	10.15	9.45	8.91	9.66	8.40	8.88	8.52	8.18	8.825
MC1	TST16	10.03	9.98	10.36	9.94	10.04	10.38	10.26	10.12	10.37	9.96	10.143
MC1	TST35	7.43	6.47	10.92	10.39	8.30	10.27	9.61	12.07	12.11	9.13	9.667
MC1	TT (60×40)	6.63	5.41	6.55	6.80	5.42	6.63	6.73	7.00	5.19	6.69	6.304
MC1	TT (50×50)	5.22	6.52	6.61	5.52	6.58	5.32	6.63	6.85	6.79	5.32	6.136
MC2	CS	6.39	6.53	6.22	6.50	6.52	6.40	6.43	6.20	5.77	6.12	6.308
MC2	CT	6.71	6.17	6.40	6.13	6.37	6.33	6.48	6.60	6.92	6.41	6.451
MC2	CTT	6.72	6.65	6.45	6.57	6.39	6.48	6.59	6.52	6.46	6.41	6.523
MC2	TST16	7.25	7.18	8.65	6.95	7.12	7.00	6.97	6.17	6.77	7.08	7.114
MC2	TST35	7.15	7.04	6.33	7.08	7.13	6.21	6.51	7.07	7.07	7.11	6.870
MC2	TT (60×40)	6.21	6.22	6.37	6.32	6.40	6.13	5.96	6.25	6.32	6.13	6.229
MC2	TT (50×50)	6.17	6.17	6.10	6.24	6.06	6.14	6.14	6.25	6.29	6.21	6.176

[1]With ratio of $d_w = 1.15 d_n$ according to [1]

Table 7 Ranks and rank sums of the Mann–Whitney U test for each comparison of MC1 and MC2

MC	DT-ID	Group	Ranks of samples 1	2	3	4	5	6	7	8	9	10	R_1, R_2
MC1	CS	1	16	15	18	11	12	19	7	9	14	17	138
MC1	CT	2	13	1	6	10	2	5	20	3	8	4	72
MC1	CS[1]	1	12	10	17	5	6	19	1	4	9	15	98
MC1	CT[1]	2	18	2	13	16	3	11	20	7	14	8	112
MC1	CS	1	17	16	19	13	14	20	11	12	15	18	155
MC1	CTT	2	10	8	1	3	4	2	7	5	6	9	55
MC1	CS	1	17	16	19	13	14	20	11	12	15	18	155
MC1	TST16	2	7	8	3	10	6	1	4	5	2	9	55
MC1	CS	1	17	16	19	12	13	20	10	11	15	18	151
MC1	TST35	2	9	14	3	4	8	5	6	2	1	7	59
MC1	CS	1	14	13	16	9	10	17	2	4	12	15	112
MC1	TT (60×40)	2	8	19	11	3	18	7	5	1	20	6	98
MC1	CS	1	13	12	15	8	9	16	1	4	11	14	103
MC1	TT (50×50)	2	20	10	6	17	7	18	5	2	3	19	107
MC1	TT (60×40)	1	8	16	12	3	15	7	5	1	20	6	93
MC1	TT (50×50)	2	19	13	10	14	11	17	9	2	4	18	117
MC2	CS	1	12	4	15	6	5	10	8	16	20	19	115
MC2	CT	2	2	17	11	18	13	14	7	3	1	9	95
MC2	CS	1	16	5	17	8	7	14	12	18	20	19	136
MC2	CTT	2	1	2	11	4	15	9	3	6	10	13	74
MC2	CS	1	15	10	16	12	11	14	13	17	20	19	147
MC2	TST16	2	2	3	1	8	4	6	7	18	9	5	63
MC2	CS	1	14	8	16	11	9	13	12	18	20	19	140
MC2	TST35	2	1	7	15	4	2	17	10	6	5	3	70
MC2	CS	1	7	1	12	3	2	5	4	15	20	18	87
MC2	TT (60×40)	2	14	13	8	9	6	17	19	11	10	16	123
MC2	CS	1	6	1	10	3	2	5	4	12	20	17	80
MC2	TT (50×50)	2	14	13	18	9	19	16	15	8	7	11	130
MC2	TT (60×40)	1	10	9	2	3	1	17	20	7	4	16	89
MC2	TT (50×50)	2	13	12	18	8	19	15	14	6	5	11	121

[1] With ratio of $d_{\mathrm{w}} = 1.15 d_{\mathrm{n}}$ according to [1]

Declarations

References

1. Guideline DVS (2016) Widerstandspunktschweißen von Stählen bis 3 mm Einzeldicke: Konstruktion und Berechnung. DVS Media 2902-3

2. Guideline (2017) Prüfen von Widerstandspressschweißverbindungen: Zerstörungsfreie Prüfung. DVS Media 2916-5

3. Füssel U, Mathiszik C, Zschetzsche J, Großmann C, Heide M (2015) Zerstörungsfreie Bewertung des Linsendurchmessers Beim Widerstandspunktschweißen Mit Magnetischen Prüfverfahren: Schlussbericht IGF-Nr. 17.539 BR/DVS-Nr. 04.058. Technische Universität Dresden, Professur für Fügetechnik und Montage, Dresden. https://doi.org/10.13140/RG.2.1.4322.9520

4. Füssel U, Mathiszik C, Zschetzsche J (2019) Zerstörungsfreie Charakterisierung der Anbindungsfläche Beim Widerstandspressschweißen Durch Bildgebende Analyse der Remanenzflussdichte: Schlussbericht IGF 19.208 B. Technische Universität Dresden, Professur für Fügetechnik und Montage, Dresden

5. Mathiszik C, Reinhardt T, Zschetzsche J, Füssel U (2018) NDT of austenitic steels - evaluation of spot weld nugget diameters by imaging analyses of the residual flux density. In: 12th ECNDT, vol. ECNDT2018. Sweden MEETX AB, Gothenburg, Sweden. https://www.ndt.net/article/ecndt2018/papers/ecndt-0478-2018.pdf

6. Mathiszik C, Zschetzsche E, Reinke A, Koal J, Zschetzsche J, Füssel U (2022) Magnetic characterization of the nugget microstructure at resistance spot welding. Crystals. 12(11):1512. https://doi.org/10.3390/cryst12111512

7. Chen J, Feng Z (2017) Online resistance spot weld NDE using infrared thermography. In: Conference on nondestructive characterization and monitoring of advanced materials, aerospace, and civil infrastructure. Proceedings of SPIE, vol 10169. Portland

8. Runnemalm A, Ahlberg J, Appelgren A, Sjökvist S (2014) Automatic inspection of spot welds by thermography. J Nondestruct Eval 33(3):398–406. https://doi.org/10.1007/s10921-014-0233-0

9. Bodnar JL, Taram A, Roquelet C, Le Noc G, Meilland P, Dupuy T, Kaczynski C, Duvaut T (2018) Assessment of nugget diameter of resistance spot welding using pulse eddy current thermography. In: Vries J, Burleigh D (eds) Thermosense: Thermal Infrared Applications XL, p 33. SPIE, Orlando, United States. https://doi.org/10.1117/12.2305080

10. Forejtova L, Zavadil T, Kolarik L, Kolarikova M, Sova J, Vavra P (2019) Non-destructive inspection by infrared thermography of resistance spot welds used in automotive industry. ACTA POLYTECHNICA. 59(3):238–247. https://doi.org/10.14311/AP.2019.59.0238

11. Andreoli AF, Chertov AM, Maev RG (2016) Correlation between peel test and real time ultrasonic test for quality diagnosis in resistance spot welding. SOLDAGEM & INSPECAO. 21(3):282–289. https://doi.org/10.1590/0104-9224/SI2103.04

12. GSI - Gesellschaft für Schweißtechnik (2005) International mbH Niederlassung SLV Duisburg: Vergleichende Untersuchung Innovativer Geräte zur Verbesserung der Schweißqual-

13. Athi N, Wylie SR, Cullen JD, Al-Shamma'a AI, Sun T (2009) Ultrasonic non-destructive evaluation for spot welding in the automotive industry. In: IEEE Sensors, 2009, pp 1518–1523. IEEE, Christchurch, New Zealand. https://doi.org/10.1109/ICSENS.2009.5398469

14. Na JK, Spencer RL (2012) Design and development of high frequency matrix phased-array ultrasonic probes. In: AIP Conference Proceedings. AIP Conference Proceedings, pp 905–912. AIP, Burlington, VT. https://doi.org/10.1063/1.4716320

15. Vogt G, Mußmann J, Vogt B, Stiller W-K (2018) Imaging spot weld inspection using phased array technology – new features and correlation to destructive testing. In: 12th ECNDT. Sweden MEETX AB, Gothenburg, Sweden

16. Roberts D, Mason J, Lewis C (2002) Ultrasonic spot weld testing with automatic classification. Sci Technol Weld Join 7(1):47–50. https://doi.org/10.1179/136217101125000532

17. Bösch L, Pasic H, Neges J, Linkenbach M (2004) Ultraschallprüfung von widerstandspunktschweißverbindungen an hochfesten stahlverbindungen im karosseriebau. In: DACH-Jahrestagung 2004. ndt.net, Salzburg

18. Bösch L, Gruber C, Neges J (2008) Vergleichsuntersuchungen mittels ultraschallprüfung, materialographie und mechanischtechnologischer prüfverfahren an widerstandspunktschweißungen unterschiedlicher verbindungsqualität. In: DACH-Jahrestagung 2008, St. Gallen

19. Denisov AA, Shakarji CM, Lawford BB, Maev RG, Paille JM (2004) Spot weld analysis with 2D ultrasonic arrays. J Res Natl Inst Stand Technol 109(2):233. https://doi.org/10.6028/jres.109.015

20. Thornton M, Han L, Shergold M (2012) Progress in NDT of resistance spot welding of aluminium using ultrasonic C-scan. NDT&E International. 48:30–38. https://doi.org/10.1016/j.ndteint.2012.02.005

21. Moghanizadeh A (2015) Ultrasonic assessment of tension shear strength in resistance spot welding. In: SPIE Smart Structures and Materials + Nondestructive Evaluation and Health Monitoring. Proc SPIE 9439. https://doi.org/10.1117/12.2076516

22. Wang X, Guan S, Hua L, Wang B, He X (2019) Classification of spot-welded joint strength using ultrasonic signal time-frequency features and PSO-SVM method. Ultrasonics. 91:161–169. https://doi.org/10.1016/j.ultras.2018.08.014

23. Zhang B, Wei Z, Osman A, Zhang X, Zhang B, Cai G, Han X, Zhou Q, Zhao Y (2018) An ultrasonic non-destructive testing method for evaluating resistance spot welding quality. In: International symposium on structural health monitoring and nondestructive testing, Saarbrücken

24. Buckley J, Servent R (2008) Improvements in ultrasonic inspection of resistance spot welds. In: The 2nd Int Conf on Technical Inspection and NDT, Tehran

25. Augner R, Loth K, Harsch K, Krauter H, Maier G (2008) Schweißverbindungsprüfung im automobilbau - entwicklung, erprobung und serienanwendung eines mobilen ultraschallminiscanners. In: DACH-Jahrestagung 2008, St. Gallen

26. Himawan R, Haryanto M, Subekti RM, Sunaryo GR (2018) Ultrasonic non-destructive prediction of spot welding shear strength. International conference on nuclear technologies and sciences (ICoNETS 2017). 962:(962). https://doi.org/10.1088/1742-6596/962/1/012047

27. Kaminski R (1999) Die Ultraschallprüfung Von Punktschweißverbindungen an Beschichteten Stahlfeinblechen und Optimierung der Schweißparameter, Hürth

28. Liu J, Xu G, Gu X, Zhou G (2015) Ultrasonic test of resistance spot welds based on wavelet package analysis. Ultrasonics. 56:557–565. https://doi.org/10.1016/j.ultras.2014.10.013

ität Beim Widerstandspunktschweißen: Abschlußbericht zum Forschungsvorhaben AiF-Nr. 13.568N (01.02.2003 - 31.1.2005)

29. Martín Ó, López M, Martín F (2007) Artificial neural networks for quality control by ultrasonic testing in resistance spot welding. J Mater Process Technol 183(2–3):226–233. https://doi.org/10.1016/j.jmatprotec.2006.10.011

30. Mozurkewich G, Ghaffari B, Potter TJ (2008) Spatially resolved ultrasonic attenuation in resistance spot welds: implications for nondestructive testing. Ultrasonics. 48(5):343–350. https://doi.org/10.1016/j.ultras.2008.01.004

31. Na JK, Gleeson ST (2013) Matrix phased array (mpa) imaging technology for resistance spot welds. In: AIP Publishing LLC (ed) 40th annual review of progress in quantitative nondestructive evaluation. AIP Conference Proceedings, pp 88–94. AIP Publishing LLC, Baltimore, Maryland, USA. https://doi.org/10.1063/1.4864806

32. Wen J, Jia H, Wang CS (2019) Quality estimation system for resistance spot welding of stainless steel. ISIJ INTERNATIONAL. 59(11):2073–2076. https://doi.org/10.2355/isijinternational.ISIJINT-2019-002

33. Zamanzad Gavidel S, Lu S, Rickli JL (2019) Performance analysis and comparison of machine learning algorithms for predicting nugget width of resistance spot welding joints. Int J Adv Manuf Technol 105(9):3779–3796. https://doi.org/10.1007/s00170-019-03821-z

34. Hamidinejad SM, Kolahan F, Kokabi AH (2012) The modeling and process analysis of resistance spot welding on galvanized steel sheets used in car body manufacturing. MATERIALS & DESIGN. 34:759–767. https://doi.org/10.1016/j.matdes.2011.06.064

35. Dilthey U, Dickersbach J (1999) Application of neural networks for quality evaluation of resistance spot welds. ISIJ INTERNATIONAL. 39(10):1061–1066. https://doi.org/10.2355/isijinternational.39.1061

36. Kim T, Lee Y, Lee J, Rhee S (2004) A study of nondestructive weld quality inspection and estimation during resistance spot welding. Key Eng Mater 270–273:2338–2344

37. El Ouafi A, Bélanger R, Méthot JF (2011) Artificial neural network-based resistance spot welding quality assessment system. Revue de Métallurgie. 108(6):343–355. https://doi.org/10.1051/metal/2011066

38. Wang X, Li Y, Meng G (2011) Monitoring of resistance spot weld quality using electrode vibration signals. Meas Sci Technol 22(4). https://doi.org/10.1088/0957-0233/22/4/045705

39. Summerville C, Compston P, Doolan M (2019) A comparison of resistance spot weld quality assessment techniques. In: Procedia Manufacturing 29 (ed) 18th International Conference on Sheet Metal, SHEMET 2019, vol 29. Leuven, pp 305–312. https://doi.org/10.1016/j.promfg.2019.02.142

40. Schlichting J, Brauser S, Pepke L-A, Maierhofer C, Rethmeier M, Kreutzbruck M (2012) Thermographic testing of spot welds. NDT&E International. 48:23–29. https://doi.org/10.1016/j.ndteint.2012.02.003

41. Bertovic M, Feistkorn S, Kanzler D, Valeske B, Vrana J (2021) Zfp 4.0 aus der sicht der zfp-community: Umfrageergebnisse, herausforderungen und perspektiven. In: DGZfP (ed) ZfP-Zeitung, pp 43–49

42. ISO 17653:2012 – Resistance welding - destructive tests on welds in metallic materials - torsion test of resistance spot welds. Beuth Verlag (2012)

43. Guideline DVS (2014) Prüfen von Widerstandspressschweißverbindungen – Zerstörende Prüfung, quasistatisch. DVS Media 2916-1

44. Großmann C (2019) Nutzung Vorhandener Standmengenpotentiale. Verschleißverringerung Durch Angepasste Elektrodenwerkstoffe und Elektrodenverschleißdiagnose Beim Widerstandspunktschweißen, Dresden

45. Pepke L-A (2014) Untersuchung der Anlagenkonfiguration Beim Widerstandspunktschweißen Von Stahlfeinblechen. epubli GmbH, Berlin

46. SEP (2011) Prüf- und Dokumentationsrichtlinie für die Fügeeignung von Feinblechen aus Stahl - Teil 2: Widerstandspunktschweißen. Verlag Stahleisen 1220-2

47. Mathiszik C, Köberlin D, Heilmann S, Zschetzsche J, Füssel U (2021) General approach for inline electrode wear monitoring at resistance spot welding. Processes 9(4):685. https://doi.org/10.3390/pr9040685

48. DIN EN ISO (2015) – Resistance welding - testing of welds - peel and chisel testing of resistance spot and projection welds. Beuth Verlag 10447

49. Guideline DVS (2021) Prüfen von Widerstandspressschweißverbindungen - Metallografische Prüfung. DVS Media 2916-4